15 MeV proton damage in NiO/β-Ga_2O_3 vertical rectifiers

IOP Publishing J. Phys. Mater. 6 (2023) 045003 https://doi.org/10.1088/2515-7639/acef98

Journal of Physics: Materials

OPEN ACCESS

RECEIVED
27 June 2023

REVISED
2 August 2023

ACCEPTED FOR PUBLICATION
10 August 2023

PUBLISHED
22 August 2023

PAPER

15 MeV proton damage in NiO/β-Ga_2O_3 vertical rectifiers

Jian-Sian Li[1], Chao-Ching Chiang[1], Xinyi Xia[1], Hsiao-Hsuan Wan[1], Jihyun Kim[2], Fan Ren[1] and S J Pearton[3,*]

[1] Department of Chemical Engineering, University of Florida, Gainesville, FL 32611, United States of America
[2] Department of Chemical and Biological Engineering, Seoul National University, Seoul 08826, Republic of Korea
[3] Department of Materials Science and Engineering, University of Florida, Gainesville, FL 32611, United States of America
[*] Author to whom any correspondence should be addressed.

E-mail: spear@mse.ufl.edu

Keywords: proton, damage, NiO, Ga_2O_3, vertical, rectifiers

Abstract

15 MeV proton irradiation of vertical geometry NiO/β-Ga_2O_3 heterojunction rectifiers produced reductions in reverse breakdown voltage from 4.3 kV to 3.7 kV for a fluence of 10^{13}ions$\cdot$cm^{-2} and 1.93 kV for 10^{14} ions$\cdot$cm^{-2}. The forward current density was also decreased by 1–2 orders of magnitude under these conditions, with associated increase in on-state resistance R_{ON}. These changes are due to a reduction in carrier density and mobility in the drift region. The reverse leakage current increased by a factor of $\sim$2 for the higher fluence. Subsequent annealing up to 400 °C further increased reverse leakage due to deterioration of the contacts, but the initial carrier density of 2.2×10^{16} cm^{-3} was almost fully restored by this annealing in the lower fluence samples and by more than 50% in the 10^{14} cm^{-2} irradiated devices. Carrier removal rates in the Ga_2O_3 were in the range 190–1200 for the fluence range employed, similar to Schottky rectifiers without the NiO.

1. Introduction

β-Ga_2O_3 is attracting significant recent attention for power switching devices [1–3] and solar-blind UV photodetectors [4]. In particular, significant advancements have been achieved in the development of NiO/β-Ga_2O_3 power rectifiers, surpassing the performance limitations observed in GaN structures, particularly in one-dimensional configurations [5–8]. Notably, the latest experimental demonstrations have shown maximum breakdown voltages exceeding 8 kV, corresponding to critical electric fields over 8 MV$\cdot$cm^{-1}. The determination of the precise critical electric field of β-Ga_2O_3 remains challenging due to its dependence on various factors such as doping in the drift region of the rectifiers, operating temperature, and geometric configuration. These factors contribute to electric field crowding, thereby influencing the critical field and necessitating further investigation.

The use of p-type NiO to form heterojunctions with n-type Ga_2O_3 has mitigated the absence of practical p-type doping for the latter. This has led to recent demonstrations of vertical rectifiers with breakdown voltages more than 8 kV with excellent high temperature operation [9]. While the device performance is promising in terms of dc and switching applications [10–26], little is known about the effects of radiation on these heterojunctions. While the Ga_2O_3 is known to be relatively resistant to total dose damage [27, 28], large reversible changes in current-voltage characteristics of the heterojunctions have been observed after Co-60 gamma ray exposure which appears to be due to conductivity changes in the NiO [29]. Other low dose ion irradiated oxides have also shown enhanced conductivity which in some cases has been linked to irradiation/illumination assisted desorption of oxygen containing species from the oxide surface [30–33]. There have also been recent demonstrations of single event burnout (SEB) in Ga_2O_3 rectifiers [34], while simulations show the SEB threshold voltage of conventional Ga_2O_3 MOSFETs is lower than that of state-of-the-art AlGaN/GaN HEMTs [35, 36]. Field management approaches can provide some mitigation of single event effects in Ga_2O_3 [37]. There is clearly scope for additional studies of radiation effects in Ga_2O_3-based device structures.

In this paper we report the effects of 15 MeV protons on the electrical performance of NiO/β-Ga_2O_3 vertical rectifiers. The displacement damage from the protons reduces the carrier concentration in the drift region of the rectifiers and reduces the breakdown voltage. Partial recovery after annealing at 400 °C is observed but is limited by degradation of the contacts.

2. Experimental

The vertical rectifiers have been described in detail previously [23–25], but in brief consist of 10 μm drift region of lightly n-type Ga_2O_3 grown on a conducting n^+ Ga_2O_3. NiO with a total thickness of 20 nm is deposited on the top surface by sputtering and contacts made to both sides by e-beam evaporation of Ti/Au to the rear surface and Ni/Au to the NiO. A schematic of the device structure is shown in figure 1.

Proton irradiations were performed at the Korean Institute of Radiological and Medical Sciences using an MC 50 (Scanditronix) cyclotron. The proton energy was held constant at 15 MeV. The irradiated fluence was either 10^{13} or 10^{14} cm^{-2} at a constant beam current of 10 nA. The irradiation times were 102 s for the low fluence and 1018 s for the high fluence. The Stopping and Range of Ions in Matter (SRIM) simulation code [38] was used to estimate the projected range of ~600 μm (figure 2, top), which means the protons end up in the conducting substrate but create damage throughout the NiO and the epitaxial Ga_2O_3 layer. We also used to the SR-NIEL simulator [39] to estimate the vacancy density distribution as a function of proton irradiation energy. The non-ionizing energy loss at this energy is 5.7×10^{-3} MeV·cm^2 g^{-1}, as shown in figure 2 (bottom) [39]. There is still a larger energy loss due to ionization, but this is dissipated as heat and does not create lattice damage. The device DC characteristics were measured with an HP 4156 parameter analyzer. Capacitance–voltage values were taken with an Agilent 4284A Precision LCR Meter. Post-irradiation annealing was carried out in a N_2 ambient for 60 s in a Rapid Thermal Annealing furnace.

3. Results and discussion

The forward current density–voltage (*J–I*) characteristics from devices after irradiation with 10^{13} cm^{-2} or 10^{14} cm^{-2} are shown in figure 3. The associated on-state resistance, R_{ON}, calculated from the slope of these are also shown. The effect of the irradiation is to reduce the forward current density by approximately one order of magnitude for the lower fluence and 2 orders of magnitude for the higher fluence. The relation between charge and electric field E (Poisson's equation) and transport (drift/diffusion) equations means that the current density depends on both carrier mobility and density, e.g.

$$J_{\text{tot}} = J_n + J_p = e\left(\mu_n n + \mu_p p\right) E$$

where n/p are the electron/hole densities, e is the electronic charge and μ is the mobility. Thus the creation of traps that remove carriers from the drift region and degrade the carrier mobility in that region are the causes of the change in forward current. Radiation creates traps that remove carriers from the conduction process and degrade mobility, i.e. n, μ are reduced [26]. The R_{ON} values show only a slight degradation for low fluence and two orders of magnitude for the high fluence. Under forward bias, the drift region conducts with an on-resistance $R_{on} = 1/ne\mu$. Therefore, a decrease in carrier density increases on-resistance. Subsequent annealing brought a partial restoration of forward current for both fluences, but degradation of the front contact was apparent above 300 °C and prevented further improvement in device performance. This is clearly a result of the Ni/Au interacting with the NiO, since previous studies have shown the rear Ti/Au/Ga_2O_3 contact is stable under these conditions [40, 41]. Control samples that were not irradiated but annealed at the same temperatures confirm the origin of the degradation at 400 °C. The trends in forward density with fluence and annealing temperature are made clearer in the linear plot of figure 4, which shows that annealing alone degrades the forward current for 400 °C anneals.

Note that companion Schottky rectifiers fabricated on the same wafer without the NiO layers also showed similar changes in current, indicating that changes in the resistance of the NiO are not responsible for the current changes. The NiO is also very highly doped ($>10^{19}$ cm^{-3}) and would not be affected at the fluences used here.

The trends in reverse current in the low bias voltage region as a function of fluence are shown in figure 5. The current increases by ~50% for the low fluence and ~100% for the higher fluence, but is further degraded by annealing, independent of whether the sample had also been irradiated. Thus, two different mechanisms are present-the introduction of generation-recombination centers by the proton damage and the contact degradation at 400 °C. The increase in current due to the contact degradation is caused by a lowering of the effective barrier height as the contact metal reacts with the Ga_2O_3 and creates a non-uniform interface [42, 43].

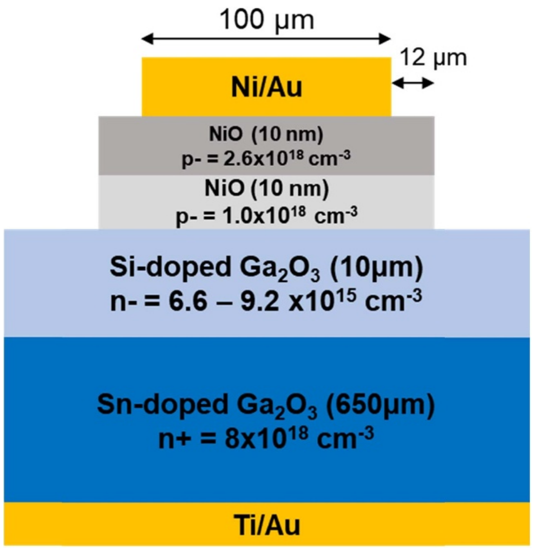

Figure 1. Schematic of heterojunction NiO/β-Ga_2O_3 rectifier.

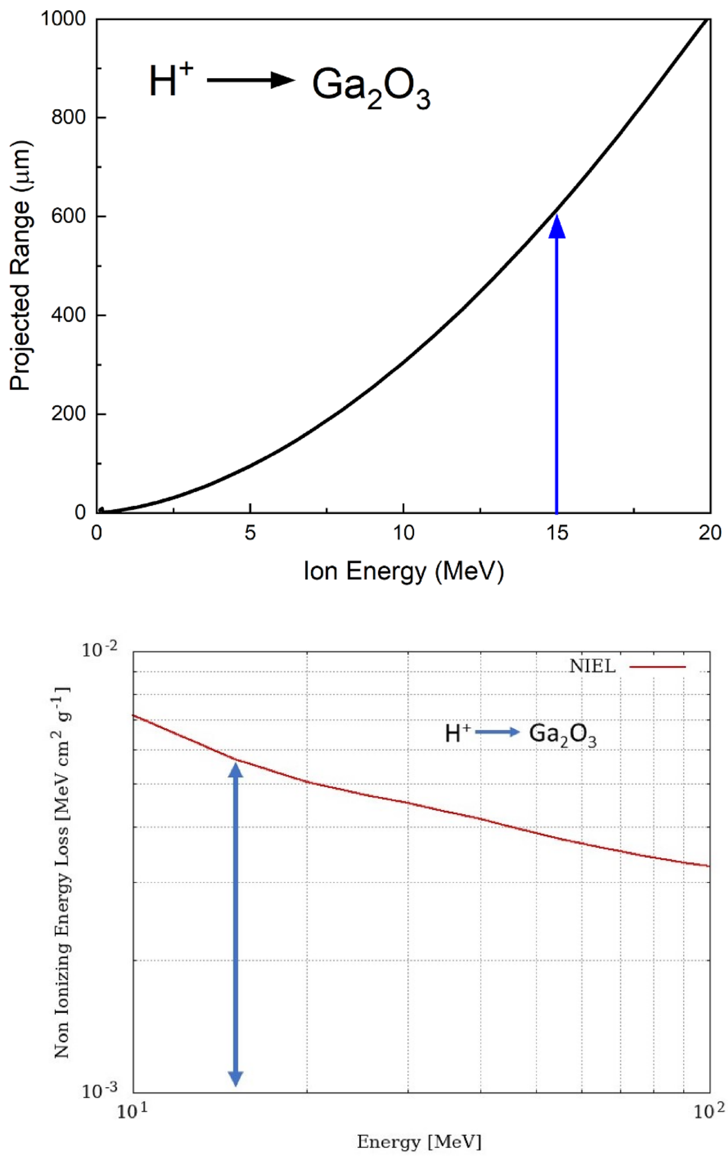

Figure 2. (Top) projected range of protons in Ga_2O_3 obtained from SRIM (bottom) NIEL of high energy protons in Ga_2O_3.

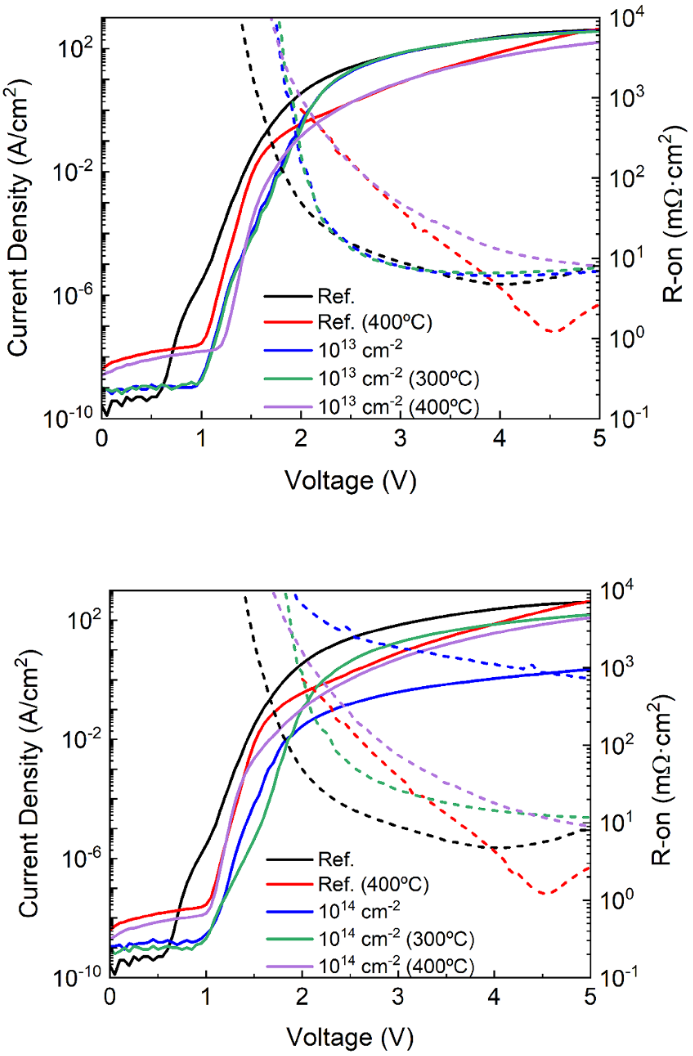

Figure 3. Forward current-density–voltage characteristics and on-state resistances from devices before and after proton irradiation and subsequent annealing for fluences of (top) 10^{13} cm^{-2} or (bottom) 10^{14} cm^{-2}.

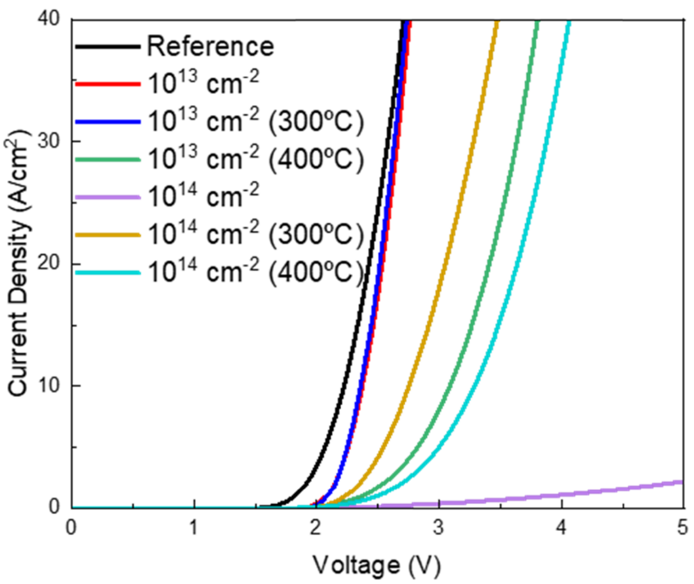

Figure 4. Combined current density–voltage characteristics from devices irradiated at both fluences and after subsequent annealing at either 300 °C or 400 °C.

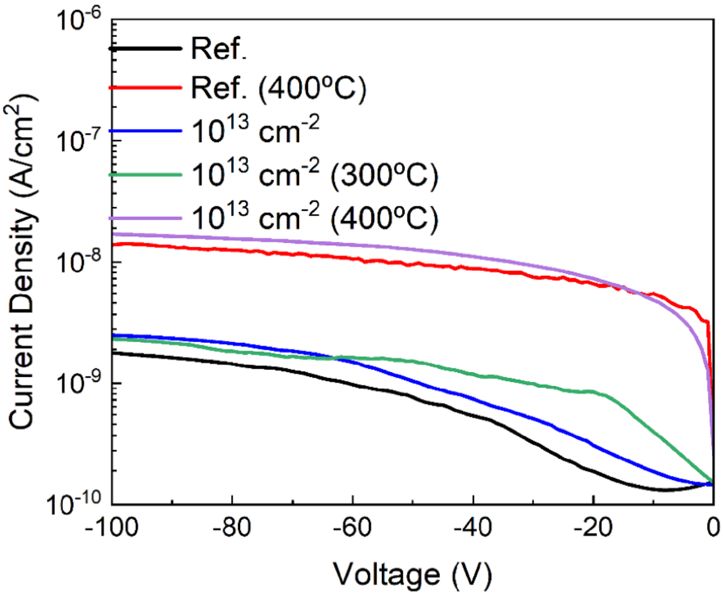

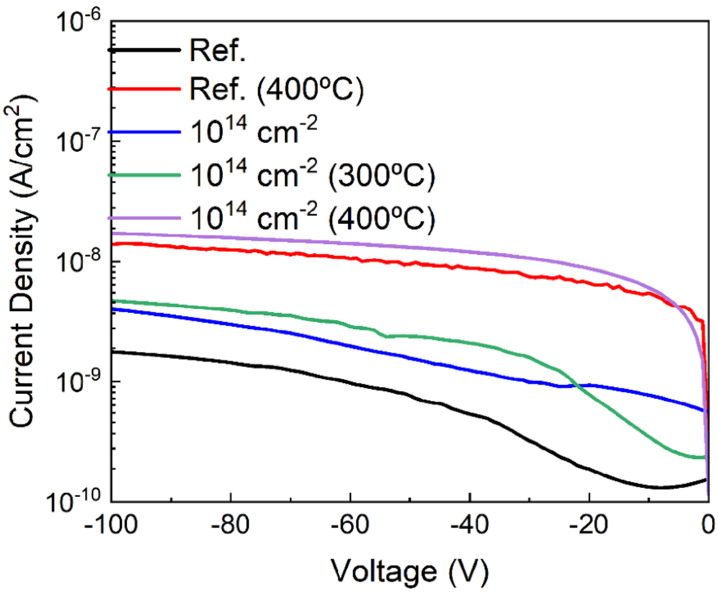

Figure 5. Low bias reverse current-density–voltage characteristics from devices before and after proton irradiation and subsequent annealing for fluences of (top) 10^{13} cm^{-2} or (bottom) 10^{14} cm^{-2}.

The breakdown voltages were extracted from the high bias reverse current characteristics and defined as the bias for a reverse current reaching 0.1 A·cm^2. These measurements were performed in Fluorinert atmosphere. As shown in figure 6, the V_B values were 4.3 kV for the unirradiated rectifiers and decreased to 3.7 kV for the low fluence and 1.93 kV for the high fluence. Annealing at 300 °C brought little change for either of the fluences but at 400 °C there was an increase to 3.7 kV for the higher fluence sample showing at this condition that the reduction in G-R centers outweighed the effect of contact degradation.

The change in drift region carrier density was obtained from the C^2–V characteristics for figure 7. The initial carrier density of 2.2×10^{16} cm^{-3} was reduced to 9.6×10^{15} cm^{-3} for the low fluence and 3.1×10^{15} for the high fluence. These reductions in carrier density do not account for the magnitude of the reduction in forward current and increase in on-state resistance, showing that carrier mobility reductions are equally important in the change of device electrical performance. Subsequent annealing at 400 °C brought a partial restoration in carrier densities, to 2.1×10^{16} and 1.7×10^{16} cm^{-3}, respectively, for the two fluences.

The carrier removal rate per ion was then obtained from the change in carrier density divided by the fluence and is included in the compilation plot of figure 8, which shows the published values for different

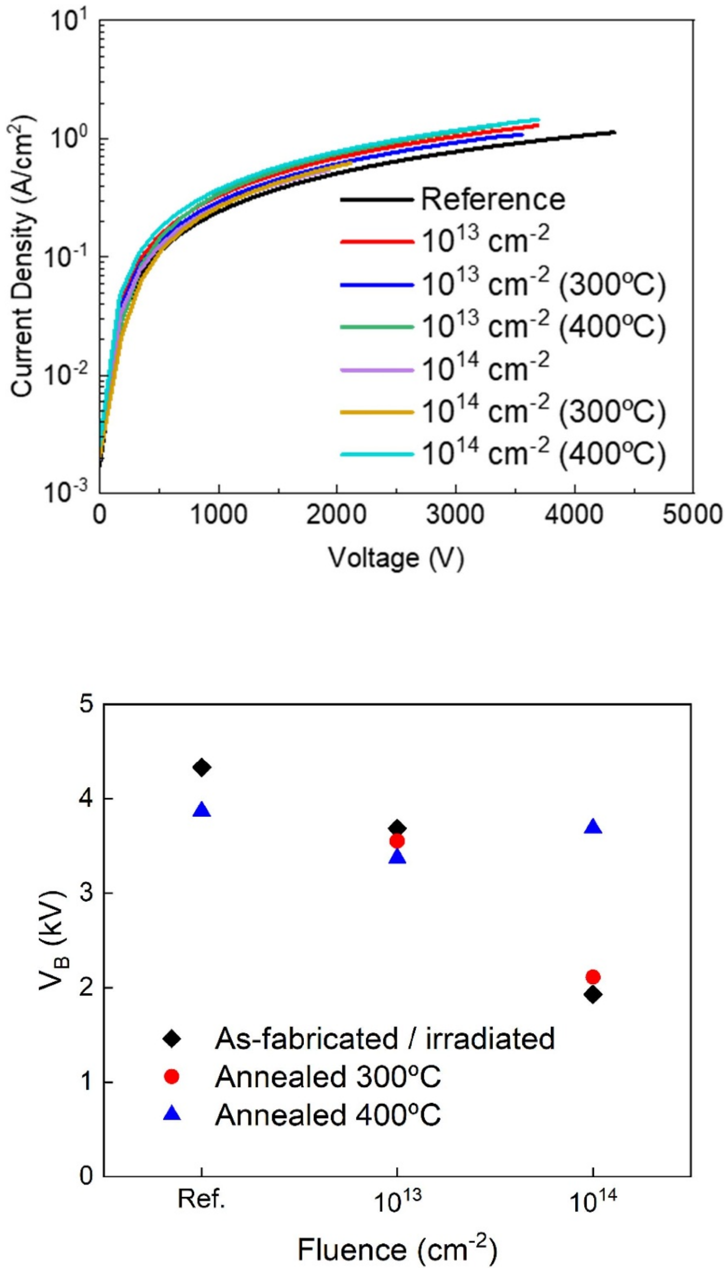

Figure 6. (Top) high bias reverse current-density–voltage characteristics from devices before and after proton irradiation and subsequent annealing for both fluences and subsequent annealing (bottom) V_B as a function of fluence and subsequent annealing temperature.

polymorphs of Ga_2O_3 irradiated with different forms of radiation [26, 27]. Since the NIEL is approximately constant over the drift layer thickness, this provides a reasonable estimate the carrier removal rate. The values obtained here for the NiO/Ga_2O_3, 1200 for 10^{13} cm^{-2} and 190 cm^{-1} for 10^{14} cm^{-2} are consistent with values reported for proton irradiation at similar energies/fluences but in Schottky diode structures that did not include the NiO [26, 27]. This indicates that in contrast to gamma irradiation [29], the heterojunction rectifiers do not show any significant differences with the presence of the NiO for proton damage. The value determined at the higher fluence may already be in the saturation region where most of the carriers are already trapped at damage sites and therefore the value at low fluence is likely to be closer to the true number.

The fact that proton damage does not produce the hysteresis in *I–V* characteristics seen for gamma irradiation in these structures indicates that the reversible resistivity changes seen in other irradiated oxides is not occurring. For example, Borgersen *et al* [30, 32] reported that irradiation of the related oxide, In_2O_3, with low doses of Si ions or and long UV exposures result in similar resistivity drops, interpreted as irradiation/illumination assisted desorption of oxygen containing species from the surface. This was consistent with the effect of post-irradiation exposure of the samples to an oxygen atmosphere partially

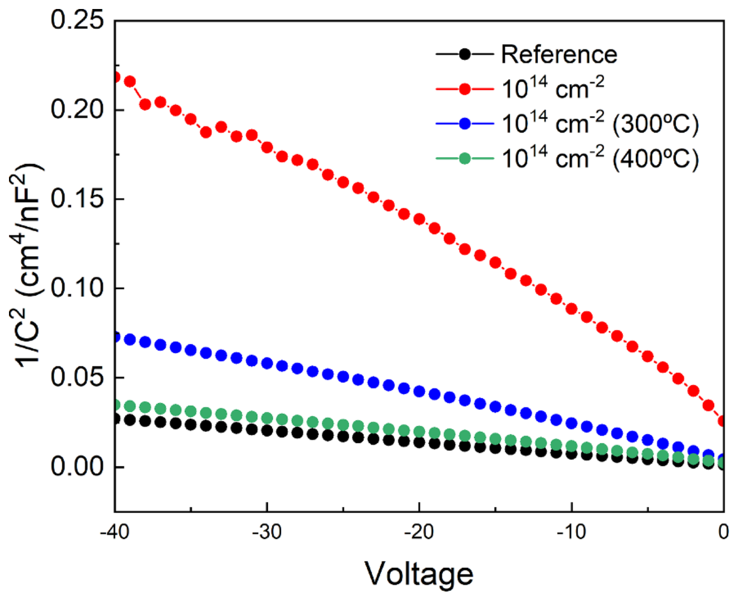

Figure 7. C^{-2}–V characteristics as a function of proton fluence and subsequent annealing temperature.

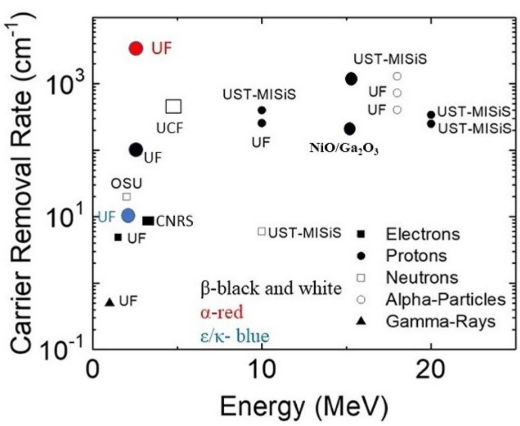

Figure 8. Compilation of carrier removal rates as a function of energy for different polytypes of Ga_2O_3 and different types of radiation.

restoring the resistivity. Swallow *et al* [33] reported that Ga_2O_3 surfaces are terminated by O–H groups, producing downward band bending and electron accumulation. Annealing to remove these hydroxyl groups converts the surface to depletion with upward band bending of 0.26 eV. In our case, the fluences of protons used here does not produce changes in the interfacial properties that affect the electrical performance of the heterojunction rectifiers.

4. Summary and conclusions

In summary, the main effects of proton irradiation on vertical geometry NiO/β-Ga_2O_3 heterojunction rectifiers were found to be a reduction in reverse breakdown voltage 4.3–3.7 kV for a fluence of 10^{13} cm^{-2} and to 1.93 kV for a fluence of 10^{14} cm^{-2}. The forward current density also decreased significantly, resulting in an increase in the on-state resistance (R_{ON}) of the rectifiers. These were due to a reduction in carrier density and mobility in the drift layer. Additionally, the reverse leakage current increased by approximately a factor of 2 for the higher fluence. Subsequent annealing at temperatures up to 400 °C further increased the reverse leakage current due to deterioration of the contacts. However, the initial carrier density was almost fully restored by this annealing process in the lower fluence samples and by more than 50% in the 10^{14} cm^{-2} irradiated devices. The carrier removal rates in the Ga_2O_3 layer were found to be in the range of 190–1200 for the employed fluence range, which is similar to Schottky rectifiers without the NiO layer.

Data availability statements

All data that support the findings of this study are included within the article (and any supplementary files).

Acknowledgments

The work at U F was performed as part of Interaction of Ionizing Radiation with Matter University Research Alliance (IIRM-URA), sponsored by the Department of the Defense, Defense Threat Reduction Agency under award HDTRA1-20-2-0002. The content of the information does not necessarily reflect the position or the policy of the federal government, and no official endorsement should be inferred. The work at U F was also supported by NSF DMR 1856662 (James Edgar). The work in Korea was supported by the Korea Institute for Advancement of Technology (KIAT) (P0012451, The Competency Development Program for Industry Specialist), the National Research Foundation of Korea (2020M3H4A3081799) and the K-Sensor Development Program (RS-2022-00154729), funded by the Ministry of Trade, Industry and Energy (MOTIE, Korea), the Institute of Civil Military Technology Cooperation Center funded by the Defense Acquisition Program Administration and Ministry of Trade, Industry and Energy, and of Korean government (20-CM-BR-05) and Korea Research Institute for defense Technology planning and advancement (KRIT) Grant funded by Defense Acquisition Program Administration (DAPA) (KRIT-CT-21-034 and KRIT-CT-22-046).

Conflict of interest

The authors have no conflicts to disclose.

ORCID iDs

Hsiao-Hsuan Wan https://orcid.org/0000-0002-6986-8217
S J Pearton https://orcid.org/0000-0001-6498-1256

References

[1] Lu X, Deng Y X, Pei Y L, Chen Z M and Wang G 2023 Recent advances in NiO/Ga_2O_3 heterojunctions for power electronics *J. Semicond.* **44** 061802
[2] Green A J *et al* 2022 β-gallium oxide power electronics *APL Mater.* **10** 029201
[3] Pearton S J, Ren F, Tadjer M and Kim J 2018 Perspective: Ga_2O_3 for ultra-high power rectifiers and MOSFETS *J. Appl. Phys.* **124** 220901
[4] Kalra A, Muazzam U U, Muralidharan R, Raghavan S and Nath D N 2022 The road ahead for ultrawide bandgap solar-blind UV photodetectors *J. Appl. Phys.* **131** 150901
[5] Sharma S, Zeng K, Saha S and Singisetti U 2020 Field-plated lateral Ga_2O_3 MOSFETs with polymer passivation and 8.03 kV breakdown voltage *IEEE Electron Device Lett.* **41** 836–9
[6] Wang C, Zhang J, Xu S, Zhang C, Feng Q, Zhang Y, Ning J, Zhao S, Zhou H and Hao Y 2021 Progress in state-of-the-art technologies of Ga_2O_3 devices *J. Phys. D: Appl. Phys.* **54** 243001
[7] Li J S, Chiang C C, Xia X, Wan H H, Ren F and Pearton S J 2023 7.5 kV, 6.2 GW cm^{-2} NiO/β-Ga_2O_3 vertical rectifiers with on–off ratio greater than 1013 *J. Vac. Sci. Technol.* A **41** 030401
[8] Zho F *et al* 2023 An avalanche-and-surge robust ultrawide-bandgap heterojunction for power electronics *Nat. Commun.* **14** 4459
[9] Zhang J *et al* 2022 Ultrawide bandgap semiconductor Ga_2O_3 power diodes *Nat. Commun.* **13** 3900
[10] Dong P, Zhang J, Yan Q, Liu Z, Ma P, Zhou H and Hao Y 2022 6 kV/3.4 mΩ·cm2 vertical β-Ga_2O_3 Schottky barrier diode with $BV^2/R_{on,sp}$ performance exceeding 1-D unipolar limit of GaN and SiC *IEEE Electron Device Lett.* **43** 765
[11] Li J-S, Chiang C-C, Xia X, Yoo T J, Ren F, Kim H and Pearton S J 2022 Demonstration of 4.7 kV breakdown voltage in NiO/β-Ga_2O_3 vertical rectifiers *Appl. Phys. Lett.* **121** 042105
[12] Liao C *et al* 2022 Optimization of NiO/β-Ga_2O_3 heterojunction diodes for high-power application *IEEE Trans. Electron Devices* **69** 5722
[13] Xiao M *et al* 2021 Packaged Ga_2O_3 Schottky rectifiers with over 60-A surge current capability *IEEE Trans. Power Electron.* **36** 8565
[14] Yan Q *et al* 2021 β-Ga_2O_3 hetero-junction barrier Schottky diode with reverse leakage current modulation and $BV^2/R_{on,sp}$ value of 0.93 GW/cm^2 *Appl. Phys. Lett.* **118** 122102
[15] Gong H H, Chen X H, Xu Y, Ren F F, Gu S L and Ye J D 2020 A 1.86 kV double-layered NiO/β-Ga_2O_3 vertical p-n heterojunction diode *Appl. Phys. Lett.* **117** 022104
[16] Gong H H *et al* 2021 β-Ga_2O_3 vertical heterojunction barrier Schottky diodes terminated with p-NiO field limiting rings *Appl. Phys. Lett.* **118** 202102
[17] Hao W, He Q, Zhou K, Xu G, Xiong W, Zhou X, Jian G, Chen C, Zhao X and Long S 2021 Low defect density and small I—V curve hysteresis in NiO/β-Ga_2O_3 pn diode with a high PFOM of 0.65 GW/cm^2 *Appl. Phys. Lett.* **118** 043501
[18] Zhou F *et al* 2022 1.95 kV beveled-mesa NiO/β-Ga_2O_3 heterojunction diode with 98.5% conversion efficiency and over million-times overvoltage ruggedness *IEEE Trans. Power Electron.* **37** 1223
[19] Yan Q, Gong H, Zhou H, Zhang J, Ye J, Liu Z, Wang C, Zheng X, Zhang R and Hao Y 2022 Low density of interface trap states and temperature dependence study of Ga_2O_3 Schottky barrier diode with p-NiO_x termination *Appl. Phys. Lett.* **120** 092106
[20] Wang Y *et al* 2022 2.41 kV vertical P-Nio/n-Ga_2O_3 heterojunction diodes with a record Baliga's figure-of-merit of 5.18 GW/cm^2 *IEEE Trans. Power Electron.* **37** 3743

[21] Wang Z *et al* 2022 Majority and minority carrier traps in NiO/β-Ga_2O_3 p^+-n heterojunction diode *IEEE Trans. Electron Devices* **69** 981
[22] Wang B, Xiao M, Spencer J, Qin Y, Sasaki K, Tadjer M J and Zhang Y 2023 2.5 kV vertical Ga_2O_3 Schottky rectifier with graded junction termination extension *IEEE Electron Device Lett.* **44** 221
[23] Li J S, Chiang C C, Xia X, Wan H H, Ren F and Pearton S J 2023 Superior high temperature performance of 8 kV NiO/ Ga_2O_3 vertical heterojunction rectifiers *J. Mater. Chem.* C **11** 7750
[24] Li J S, Wan H H, Chiang C C, Xia X, Yoo T, Kim H, Ren F and Pearton S J 2023 Reproducible NiO/Ga_2O_3 vertical rectifiers with breakdown voltage $>$ 8 kV *Crystals* **13** 886
[25] Li J S, Chiang C C, Xia X, Wan H H, Ren F and Pearton S J 2023 Effect of drift layer doping and NiO parameters in achieving 8.9 kV breakdown in 100 μm diameter and 4 kV/4A in 1 mm diameter NiO/Ga_2O_3 rectifiers *J. Vac. Sci. Technol.* A **41** 043404
[26] Kim J, Pearton S J, Fares C, Yang J, Ren F, Kim S and Polyakov A Y 2019 Radiation damage effects in Ga_2O_3 materials and devices *J. Mater. Chem.* C **7** 10
[27] Xia X *et al* 2022 Radiation damage in the ultra-wide bandgap semiconductor Ga_2O_3 *ECS J. Solid State Sci. Technol.* **11** 095001
[28] Wong M H, Takeyama A, Makino T, Ohshima T, Sasaki K, Kuramata A, Yamakoshi S and Higashiwaki M 2018 Radiation hardness of β-Ga_2O_3 metal-oxide-semiconductor field-effect transistors against gamma-ray irradiation *Appl. Phys. Lett.* **112** 023503
[29] Li J-S, Chiang C-C, Xia X, Stepanoff S, Haque A, Wolfe D E, Ren F and Pearton S J 2023 Reversible total ionizing dose effects in NiO/Ga_2O_3 heterojunction rectifiers *J. Appl. Phys.* **133** 015702
[30] Borgersen J, Karsthof R, Rønning V, Vines L, von Wenckstern H, Grundmann M, Kuznetsov A Y and Johansen K M 2023 Origin of enhanced conductivity in low dose ion irradiated oxides *AIP Adv.* **13** 015211
[31] Borgersen J, Vines L, Frodason Y K, Kuznetsov A, von Wenckstern H, Grundmann M, Allen M, Zúñiga-Pérez J and Johansen K M 2020 Experimental exploration of the amphoteric defect model by cryogenic ion irradiation of a range of wide band gap oxide materials *J. Phys.: Condens. Matter* **32** 415704
[32] Borgersen J, Johansen K M, Vines L, von Wenckstern H, Grundmann M and Kuznetsov A Y 2021 Fermi level controlled point defect balance in ion irradiated indium oxide *J. Appl. Phys.* **130** 085703
[33] Swallow J E N, Varley J B, Jones L A H, Gibbon J T, Piper L F J, Dhanak V R and Veal T D 2019 Transition from electron accumulation to depletion at β-Ga_2O_3 surfaces: the role of hydrogen and the charge neutrality level *APL Mater.* **7** 022528
[34] Cadena R M *et al* 2023 Low-energy ion-induced single-event burnout in gallium oxide Schottky diodes *IEEE Trans. Nucl. Sci.* **70** 363
[35] Ma H, Wang W, Cai Y, Wang Z, Zhang T, Feng Q, Chen Y, Zhang C, Zhang J and Hao Y 2023 Analysis of single event effects by heavy ion irradiation of Ga_2O_3 metal–oxide–semiconductor field-effect transistors *J. Appl. Phys.* **133** 085701
[36] Datta A and Singisetti U 2023 Simulation studies of single event effects in b-Ga_2O_3 MOSFETs *IEEE Trans Nucl. Sci.* accepted
[37] Sharma R, Li J S, Law M E, Ren F and Pearton S J 2023 Effect of biased field rings to improve charge removal after heavy-ion strikes in vertical geometry β-Ga_2O_3 rectifiers *ECS J. Solid State Sci. Technol.* **12** 035003
[38] Ziegler J F Interaction of Ions with Matter (available at: www.srim.org/index.htm)
[39] Boschini M J, Rancoita P G and Tacconi M 2014 SR-NIEL-7 calculator: screened relativistic (SR) treatment for calculating the displacement damage and nuclear stopping powers for electrons, protons, light- and heavy-ions in materials (version 9.3); website currently supported within the space radiation environment activities of ASIF (ASI—Italian Space Agency-Supported Irradiation Facilities) (available at: www.sr-niel.org/) (June 2023)
[40] Lyle L A M 2022 Critical review of Ohmic and Schottky contacts to β-Ga_2O_3 *J. Vac. Sci. Technol.* A **40** 060802
[41] Sheoran H, Kumar V and Singh R 2022 A comprehensive review on recent developments in Ohmic and Schottky contacts on Ga_2O_3 for device applications *ACS Appl. Electron. Mater.* **4** 2589
[42] Lee M-H, Chou T-S, Bin Anooz S, Galazka Z, Popp A and Peterson R L 2022 Effect of post-metallization anneal on (100) Ga_2O_3/Ti–Au ohmic contact performance and interfacial degradation *APL Mater.* **10** 091105
[43] Lee M-H, Chou T-S, Bin Anooz S, Galazka Z, Popp A and Peterson R L 2022 Exploiting the nanostructural anisotropy of β-Ga_2O_3 to demonstrate giant improvement in titanium/gold Ohmic contacts *ACS Nano* **16** 11988–97